Response of Systems and Components in a Base-Isolated Nuclear Power Plant Building Impacted by a Large Commercial Aircraft

Manish Kumar, M.ASCE[1]; and Andrew Whittaker, F.ASCE[2]

Abstract: Earthquake shaking must be addressed in the design of a nuclear power plant (NPP). The impact of a large commercial airliner on a nuclear power plant building is considered a beyond-design-basis event but assessment is required for new reactors. This paper investigates the effect of beyond-design-basis impact of a large commercial airliner on a base-isolated NPP constructed to resist the effects of design-basis earthquake shaking. A finite element model of the testbed NPP is analyzed for design-basis shaking at a site of high seismic hazard and for aircraft impact. Spectral demands on systems and components inside but not attached to the containment vessel are compared for (1) design-basis shaking of the conventionally constructed testbed; (2) design-basis shaking of the base-isolated testbed; and (3) aircraft impact loading of the base-isolated testbed. The importance of isolation-system parameters, soil-structure-interaction (SSI), and soil modeling on the impact-related spectral demands of the isolated NPP are investigated and reported. Elastic material behavior is assumed for the superstructure and the soil, and nonlinear hysteretic behavior is assumed for the lead-rubber isolation system. For the assumed aircraft impact, the installation of a seismic isolation system increases in-structure spectral demands on structures, systems, and components inside containment with respect to the fixed-base condition. In-structure spectral demands due to aircraft impact in a base-isolated NPP are insensitive to the secant period and/or characteristic strength of the isolation system. The effect of soil-structure interaction on the impact response is significant for the fixed-base NPP but relatively small for the base-isolated NPP. DOI: 10.1061/(ASCE)ST.1943-541X.0002155. © 2018 American Society of Civil Engineers.

Introduction

Seismic isolation using low damping rubber (LDR), lead–rubber (LR), and friction pendulum bearings is a viable strategy for mitigating the effects of extreme earthquake shaking on safety-related nuclear structures. A study supported by the United States Nuclear Regulatory Commission (USNRC) investigated the effect of design and beyond-design earthquake shaking on base-isolated nuclear power plants (NPPs) (e.g., Kumar et al. 2015a, b, c, d, e; Kumar et al. 2014) and formulated draft design guidance to achieve specific performance goals at the plant level.

The USNRC defines the impact of large commercial aircraft on a NPP as a beyond-design-basis event. A plant-specific assessment of aircraft impact is required per 10 CFR Part 50 (USNRC 1998a) and Part 52 (USNRC 1998b) for new reactors. This paper addresses the effects of impact of a large commercial aircraft on systems and components in a testbed NPP. Results are reported from analysis of the testbed to help judge whether the introduction of an isolation system, which dramatically improves performance in design-basis and beyond-design-basis earthquake shaking, negatively impacts response under beyond-design-basis aircraft impact.

There are many factors that affect the impact-induced response of systems and components inside a NPP, including (1) size, mass, and stiffness of the NPP; (2) the size, mass, and velocity of the impacting aircraft; (3) the point and orientation of aircraft impact on the NPP; (4) the mechanical properties of the isolation system (if used); (5) soil-structure-interaction; and (6) soil stiffness and damping. Factors 3–6 are investigated in this paper for a testbed NPP impacted by a large commercial airliner at high speed. Although the quantitative results are somewhat specific to the testbed NPP and impact regime, the process presented in this paper could be followed for a project-specific investigation of demands on structures, systems, and components in a base-isolated NPP resulting from beyond-design-basis aircraft impact.

The effect of aircraft impact on fixed-base NPPs has been studied. Much of seminal research was performed by Riera (1968) who proposed a methodology to obtain the load history for aircraft impact on a NPP, now widely known as the Riera loading function. Riera (1980) reported peak values of in-structure spectral accelerations associated with aircraft impact were expected in the frequency range of 8–40 Hz, and that maximum values would exceed those due to design-basis earthquake shaking at frequencies greater than 10 Hz. Since that time, both the physical size and the impact velocity of the aircraft considered for analysis have increased. (For most NPP sites in the United States, the intensity of design-basis earthquake shaking has also increased since 1980).

Load histories for impact of commercial aircraft have been derived for a range of scenarios (e.g., Kostov et al. 2013; Iliev et al. 2013). Simplified and advanced numerical techniques have been employed to obtain in-structure response spectra in fixed-base nuclear power plant buildings due to aircraft impact (e.g., Andonov et al. 2009, 2010; Kirkpatrick et al. 2013; Arros and Doumbalski 2007). Values of in-structure spectral acceleration at higher frequencies are very sensitive to the numerical techniques

[1]Assistant Professor, Dept. of Civil Engineering, Indian Institute of Technology Bombay, Mumbai, Maharashtra 400076, India (corresponding author). ORCID: https://orcid.org/0000-0002-2582-1900. Email: mkumar@iitb.ac.in

[2]Professor, Dept. of Civil, Structural and Environmental Engineering, State Univ. of New York, Buffalo, NY 14260.

Note. This manuscript was submitted on October 12, 2017; approved on March 28, 2018; published online on July 2, 2018. Discussion period open until December 2, 2018; separate discussions must be submitted for individual papers. This paper is part of the Journal of Structural Engineering, © ASCE, ISSN 0733-9445.

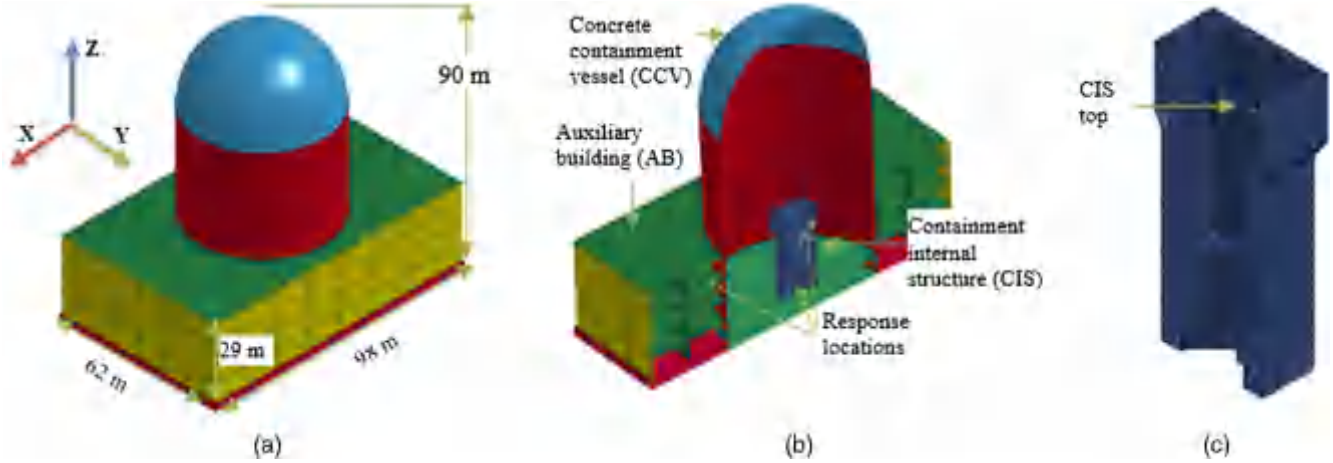

Fig. 1. Finite element model of the archetype NPP: (a) dimensions; (b) NPP sectional view; and (c) CIS.

(e.g., choice of integrators, methods used to implement damping) employed to calculate response. Importantly, the artificially sharp corners on the load-history functions introduce high frequency noise (Andonov et al. 2009). Although some designs have been based on enveloped Riera load histories, Andonov et al. (2009) reported that this practice, for a given aircraft and range of fuel weight and impact velocity, did not necessarily provide conservative (high) estimates of in-structure floor spectra.

Kulak and Yoo (2003) analyzed a base-isolated NPP impacted by aircraft but used a single degree of freedom (SDOF) representation of the reactor building and a simplified Riera loading function, without consideration of the location of the impact or the mechanical properties of the isolation system. Keldrauk et al. (2011) performed parametric analysis with varying isolation period and mass of the superstructure to estimate the response of base-isolated NPP subject to aircraft impact. They concluded that acceleration response is not sensitive to the isolation period but increases when superstructure mass is reduced: an intuitive observation supported by simple dynamics calculations. These authors assumed linear elastic isolators with 10% damping and modeled the NPP as a three-story shear structure for their calculations.

A finite element (FE) model of an archetype large light water NPP is used here to investigate the effects of impact of a large commercial aircraft on the containment vessel of a base-isolated NPP. The study focuses on the systems and components inside but not physically attached to the containment vessel. Breach of the containment vessel due to aircraft impact is not addressed because this outcome would be independent of support conditions (i.e., isolation system, flexible soil, and rigid base). Results of seismic and impact analysis are presented and compared. Earthquake analysis is performed assuming the testbed NPP is sited in a region of high seismic hazard. The impact analysis assumes high-speed strike of a large commercial airliner on the containment vessel of the testbed NPP.

Reactor Model

A FE model of the representative NPP described in Orr (2003) was created in LS-DYNA. This NPP consists of an auxiliary building (AB), a concrete containment vessel (CCV), and a containment internal structure (CIS), all sharing a common basemat. The CIS is joined only to the basemat and the AB is joined to the CCV. The AB and CCV are modeled using shell elements, and the CIS and basemat are modeled using solid elements. Linear elastic properties for concrete and steel materials are assumed. Safety-critical systems and components are attached to the CIV and not to the CCV per conventional practice.

The response of the CCV due to aircraft impact is assumed linear for the analyses reported in this paper. Although local nonlinear behavior, including spalling and scabbing of concrete, might be expected in the event of aircraft impact, reducing the energy imparted to the remainder of the NPP building, it cannot be quantified for this CCV because reinforcement details are not available. Importantly, the time scales for local damage to the CCV and global response of the NPP and CIS are very different. Local damage to the CCV, if any, will occur in the milliseconds after impact whereas global response of the NPP and the CIS will begin tens to hundreds of milliseconds after impact: an outcome related to the compressional wave speed in reinforced concrete.

The total mass of the NPP, including the basemat, is 155,000 tons. The dimensions and sectional views of the NPP and the locations where responses are shown in Fig. 1. Modal properties of the NPP are presented in Fig. 2. The first two horizontal modes (Modes 1 and 2) are vibration of the AB and the CCV in the horizontal directions. The following two horizontal modes (Modes 9 and 10) are vibration of the CIS. Mode 16 is vertical vibration of the AB.

Isolation System

The NPP is isolated on a common basemat slab using a symmetrical layout of 273 LR bearings. The dimensions of the reinforced concrete basemat are $98 \times 62 \times 2.5$ m. LS-DYNA provides a direct option to model elastomeric bearings through a material model *MAT_SEISMIC_ISOLATOR. The corresponding isolator element and sectional properties are defined using options *ELEMENT_BEAM and *SECTION_BEAM, respectively. ELFORM is set to 6 (discrete beam), and the local axes of the isolator is defined in *SECTION_BEAM option. Behavior in the two horizontal (shear) directions is based on the model proposed by Park et al. (1986) and extended for seismic isolators by Nagarajaiah et al. (1989). The vertical stiffness for all types of isolators is linear elastic, with the option to provide different values in compression and tension. The element has no rotational or torsional stiffness and a pinned joint is assumed. Moments are calculated as the product of

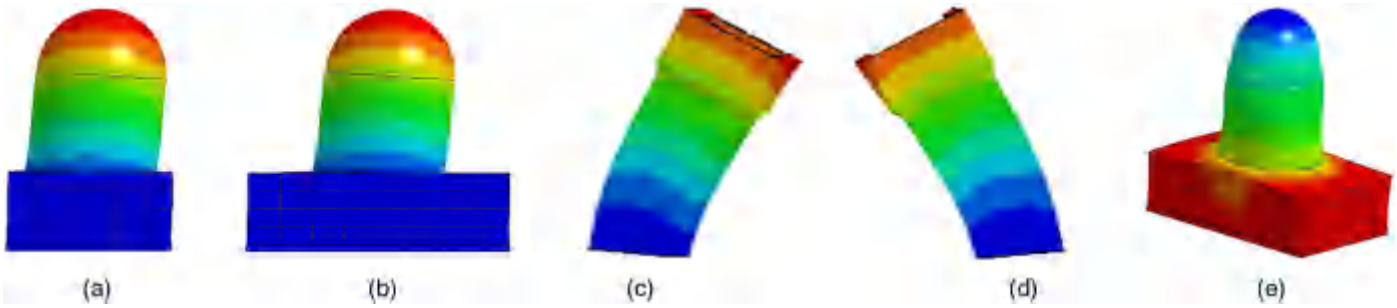

Fig. 2. Modal responses of the model of the NPP: (a) Mode 1 (f ¼ 3.47 Hz); (b) Mode 2 (f ¼ 3.62 Hz); (c) Mode 9 (f ¼ 7.02); (d) Mode 10 (f ¼ 7.02); and (e) Mode 16 (f ¼ 8.96 Hz).

Table 1. Geometrical and mechanical properties of elastomeric bearings

		T ¼ 2 s	T ¼ 3 s	
Property	Notation	Q_d=W ¼ 0.12	Q_d=W ¼ 0.12	Q_d=W ¼ 0.12
Single rubber layer thickness	t_r (mm)	10	10	10
Number of rubber layers	n	31	31	31
Steel shim thickness	t_s (mm)	4.75	4.75	4.76
Outer diameter	D_o (mm)	1,548	1,548	1,532
Inner/lead core diameter	D_i (mm)	317	317	224
Rubber cover thickness	t_c (mm)	25	25	25
Shear modulus	G (MPa)	0.94	0.42	0.42
Bulk modulus of rubber	K_{bulk} (MPa)	2,000	2,000	2,000
Yield stress of lead	σ_L (MPa)	8.5	8.5	8.5
Horizontal yield displacement	u_y (mm)	21	21	21
Static pressure due to gravity loads	p_{static} (MPa)	3.0	3.0	3.0

the vertical load and the lateral displacement of the isolator and distributed between the two nodes by assigning moment factors [The moment associated with the shearing force and the height of the isolator is not addressed but that does not significantly affect isolator response, as presented in Kumar and Whittaker (2017)]. Additional details on modeling a seismic isolator using *MAT_SEISMIC_ISOLATOR is provided in LS-DYNA User's Manual (LSTC 2017a). The advanced model of the lead-rubber bearing per Kumar et al. (2014) was not required for these analyses because the horizontal deformation demands were small, as described subsequently.

The geometric and mechanical properties of the LR bearings used for the analysis are summarized in Table 1. The procedure to obtain these properties is described in Kumar et al. (2015c). Most of the analyses were performed with the isolation system with a ratio of characteristic strength to supported weight, Q_d=W, equal to 0.12. In this table, (1) the reported period, T, is that associated with the flexibility of the elastomer, and not the secant stiffness to expected maximum displacement; and (2) the characteristic strength, Q_d, is normalized by the supported weight. The assumed bilinear hysteresis of the LR bearing is described in Fig. 3.

Damping

A Rayleigh damping formulation was used for the superstructure and the isolators. The superstructure was assigned a mass damping of 4% based on its first horizontal frequency and a damping of 4% using a stiffness damping formulation defined in LS-DYNA that uniformly damps all the high frequency modes (LSTC 2016). Isolators were assigned a mass damping of 2% based on the horizontal isolation frequency and 2% stiffness damping. The mass and stiffness damping assigned to the isolators supplemented the hysteretic damping provided by the LR bearings due to energy dissipation in the lead cores.

Analysis Cases

Fixed and base-isolated models of NPPs were analyzed for aircraft and design-basis earthquake loadings. The effects on response of the isolation period and normalized characteristic strength were investigated. Two locations of impact were considered. The effects of soil-structure interaction on the predicted response of the NPP to aircraft impact were also characterized.

Results of the seismic and impact analysis are reported here for the horizontal direction (X and Y) only. The direction of aircraft

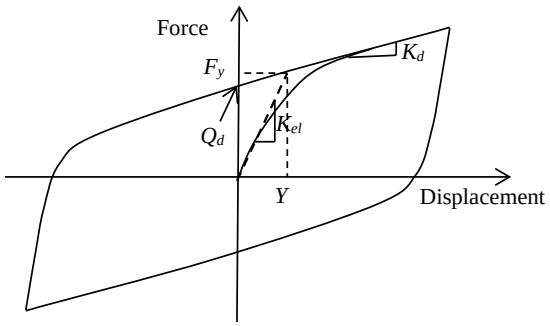

Fig. 3. Mathematical model of lead rubber bearing in the horizontal (shear) direction.

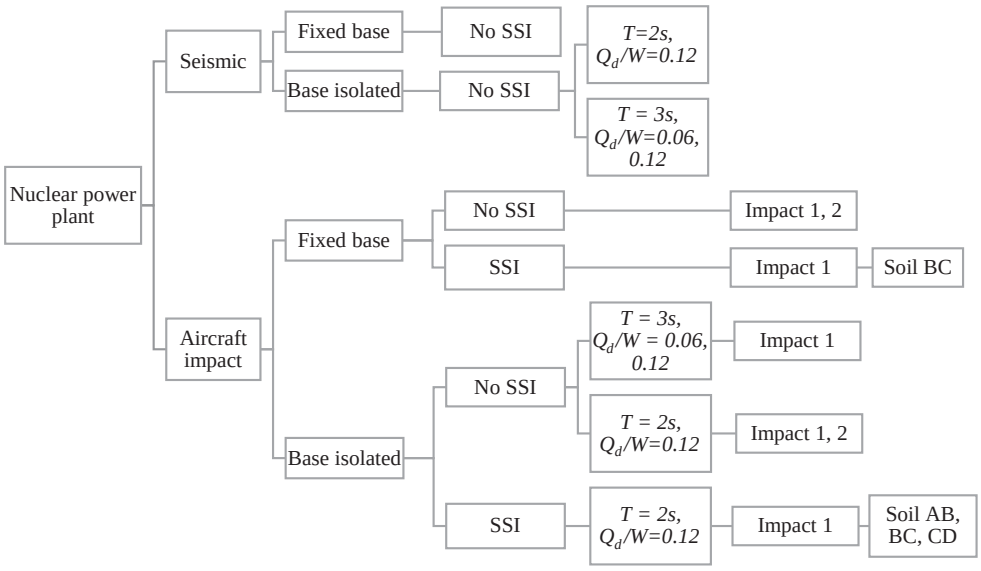

Fig. 4. Cases considered for the analysis of NPP.

impact is along the X-axis, as shown in Fig. 1. Results of the analyses in the Z (vertical) direction are substantially influenced by the treatment of damping in this direction. The analysis cases considered for this study are presented in Fig. 4. The benchmark results presented in this paper, unless noted otherwise, were obtained for a NPP with isolation system of T ¼ 2 s, Q_d=W ¼ 0.12, a site described by the boundary between soil types B and C per ASCE 7-10 (ASCE 2010), 5% critical damping in the soil, and impact Location 1 (Fig. 11).

Seismic Response-History Analysis

The response-history analyses of the NPPs were performed using 30 sets of three-component ground motions selected and then spectrally matched to be consistent with uniform hazard response spectra (UHRS) for design-basis earthquake shaking at the site of the Diablo Canyon Nuclear Generating Station: a site of high seismic hazard in the United States and the location of two operating nuclear reactors. The UHRS was calculated assuming a return period of 10,000 years. Complete details on the ground motions are presented in Kumar et al. (2015e). One of the 30 three-component sets of scaled ground motions (NGA 72, Lake Hughes, 1971 San Fernando earthquake) was used here to perform nonlinear response-history analysis. The 5% damped acceleration response spectra in the two horizontal and the vertical direction are shown in Fig. 5, and closely match the target spectra, enabling a comparison of in-structure response spectra for design-basis earthquake shaking and beyond design-basis aircraft impact. Soil-structure-interaction was not considered for the seismic analysis of the base-isolated NPP because the lateral flexibility of the isolation system will substantially reduce or eliminate its effect.

The in-structure (floor) response spectra at the center of the basemat, top of the CIS, and third floor of the auxiliary building in the fixed-base and base-isolated NPPs, are presented in Figs. 6–8, respectively (see Fig. 1 for the monitoring locations). Base isolation of the NPP substantially reduces its seismic response in the horizontal directions at all monitoring locations. The relatively large floor response in the isolated auxiliary building of Fig. 8(a) is due to the local flexibility of the floor slab and the coupling of vertical and horizontal modes of response.

Aircraft Impact Analysis

Riera (1968) proposed a force history for the normal impact of an aircraft on a rigid reflecting surface:

$$F_x(t) = P_c + \rho v^2 \qquad (1)$$

where P_c = axial buckling or crushing strength of the aircraft fuselage; ρ = mass density; and v = impact velocity. Dynamic

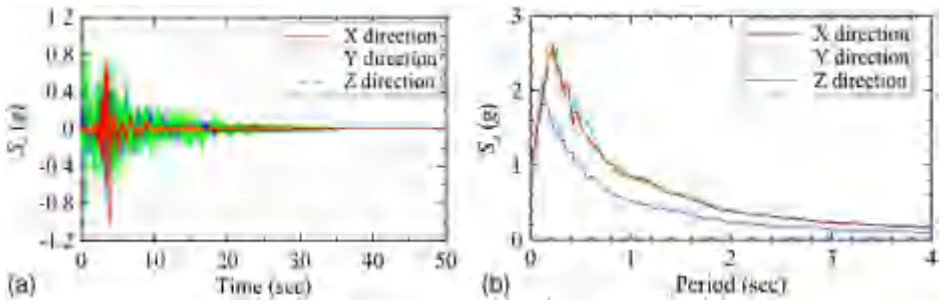

Fig. 5. Surface free field acceleration histories and response spectra for the NGA 72 ground motion scaled to the design-basis earthquake, Diablo Canyon Nuclear Generating Station, site class B-C: (a) acceleration histories; and (b) response spectra.

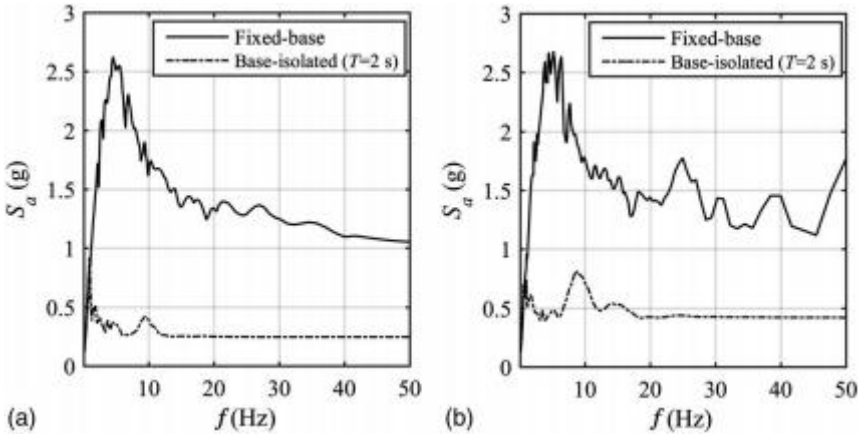

Fig. 6. In-structure response spectra at the center of basemat. Design-basis earthquake shaking, no SSI: (a) X direction; and (b) Y direction.

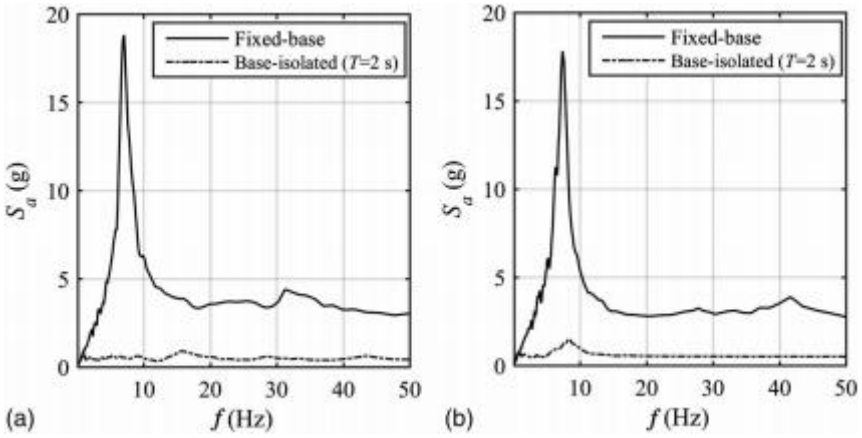

Fig. 7. In-structure response spectra at the top of the CIS: design-basis earthquake shaking, no SSI: (a) X direction; and (b) Y direction.

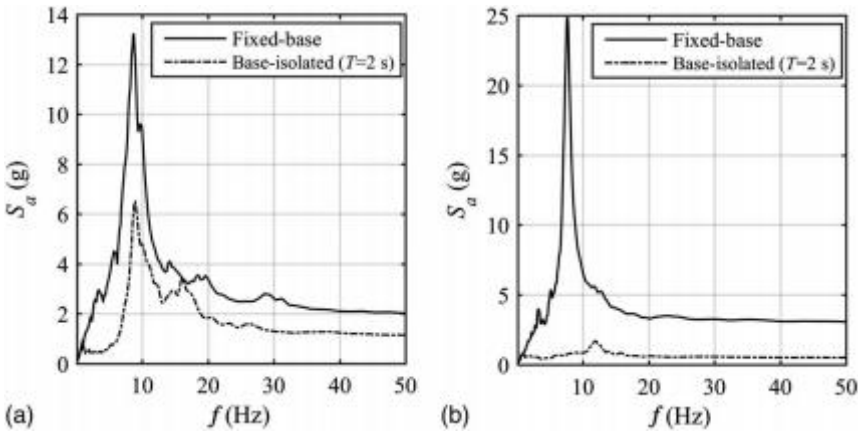

Fig. 8. In-structure response spectra at the 3rd floor of the auxiliary building. Design-basis earthquake shaking, no SSI: (a) X direction; and (b) Y direction.

interaction of the structure and the aircraft is ignored. The accuracy of the load history obtained using Eq. (1) depends on the validity of two assumptions: (1) the target is rigid and the orientation of the impact is such that the fuselage buckles axially; and (2) the distribution of mass (ρ) and the crushing strength (P_c) of the fuselage along its axis. For oblique impact and non-rigid targets, the amplitude of the force obtained using Eq. (1) is conservative (Riera 1980).

Riera load histories have been developed for a number of commercial aircraft. The key parameters are the mass density and axial crushing strength of the aircraft. The load history is applied over an assumed area of impact. The area over which the load is applied can

be assumed equal to the average cross-sectional area of fuselage. Passenger aircraft are categorized into three groups based on their size and mass (Andonov et al. 2010), as presented in Table 2.

The impact of a Boeing 747-400 is considered here using the loading history of Iliev et al. (2011). The impact velocity is assumed to be 120 m=s. An impact area of 100 m^2 is used, which is the average cross-section area of the fuselage and the wing, as shown in Fig. 9.

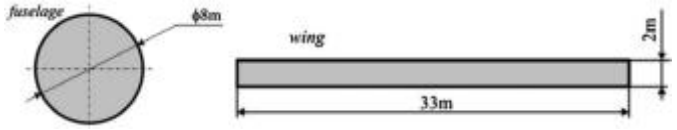

Fig. 9. Effective area of impact for the Boeing 747-400 aircraft. (Data from Iliev et al. 2011.)

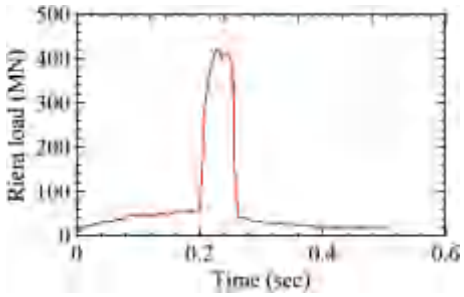

Fig. 10. Riera function for a B747-400.

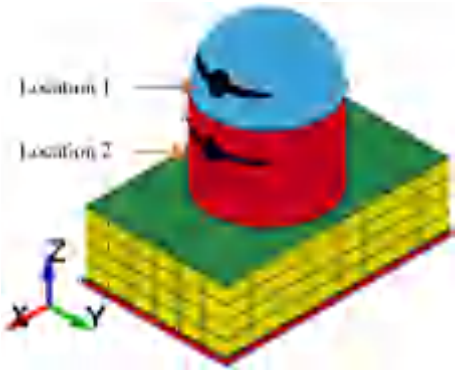

Fig. 11. Assumed locations of aircraft impact.

The Riera function for B747-400 at an impact velocity of 120 m=s is presented in Fig. 10. Two impact locations were considered for analysis of the NPP, as shown in Fig. 11: (1) Location 1, 71 m above basemat, at the mid-height of the dome of the containment vessel, and (2) Location 2, 48 m above basemat, at the 3/4 height of the cylindrical part of the containment vessel, above the roof of auxiliary building. The impact loading was applied to the model as a pressure vector perpendicular to individual shell elements across the projected cross-sectional area of the fuselage.

The in-structure response spectra in the direction of loading (X) for impact at Location 1, in the fixed-base and base-isolated NPPs are presented in Fig. 12. Neither model includes soil below the building. The energy of the impact is transferred through the CCV and the attached auxiliary building to the ground, which results in high accelerations in these components of the structure. Small floor accelerations are calculated for the basemat of the fixed-base NPP and in the containment internal structure because of the assumed boundary conditions. In the isolated NPPs, the entire building is set in motion by the impact, generating significant spectral accelerations on the basemat and in the containment internal structure. The spectral accelerations in the auxiliary building, at the location chosen to report results, are not changed substantially by the installation of the isolation system. The period of the isolation system has no significant effect on the in-structure response spectra.

The in-structure response spectra in the base-isolated NPPs for aircraft impact at Location 1 and design-basis earthquake shaking are presented in Fig. 13. The spectral accelerations due to aircraft impact are greater than those associated with design-basis earthquake shaking at moderate and high frequencies.

The effect of location of impact on the response of the NPP is investigated next. In-structure response spectra for the two locations of impact are presented in Fig. 14. The spectral demands at high frequencies are smaller for the impact closer to the basemat (i.e., Location 2).

The response of the fixed-base NPP due to aircraft impact is benchmarked against the seismic response of the corresponding base-isolated NPP in Fig. 15. The spectral demands due to aircraft impact in the fixed-base NPP are greater than those associated with design-basis earthquake shaking for the base-isolated NPPs at frequencies less than 10 Hz. The horizontal responses of one of the isolators (T ¼ 2 s, Q_d=W ¼ 0.12) for aircraft impact at Location 1 and for design-basis earthquake shaking are presented in

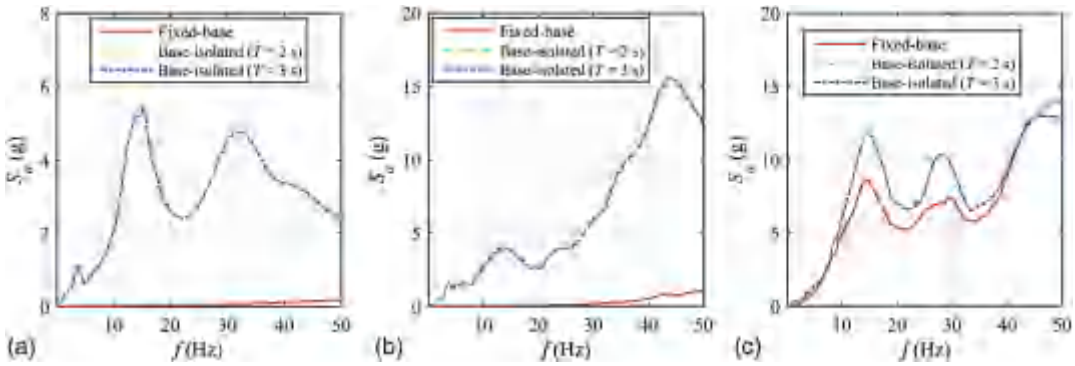

Fig. 12. In-structure response spectra (X direction) due to aircraft impact at Location 1, no SSI: (a) basemat; (b) containment internal structure; and (c) auxiliary building.

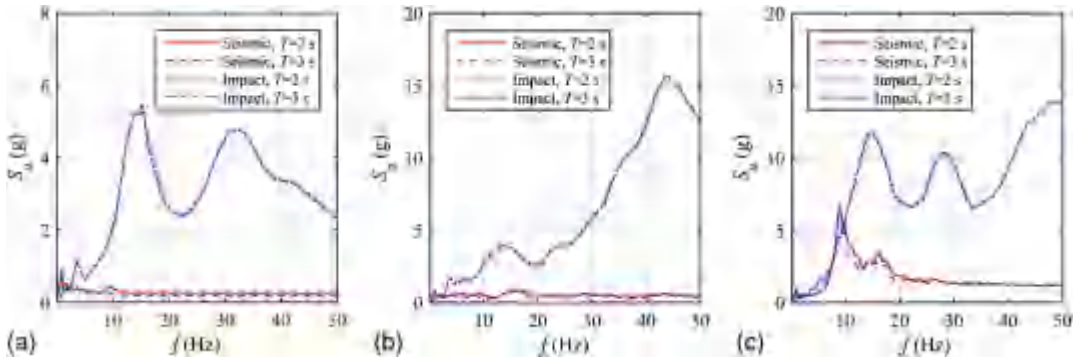

Fig. 13. In-structure response spectra (X direction) in the base-isolated nuclear power plants, no SSI: (a) basemat; (b) containment internal structure; and (c) auxiliary building.

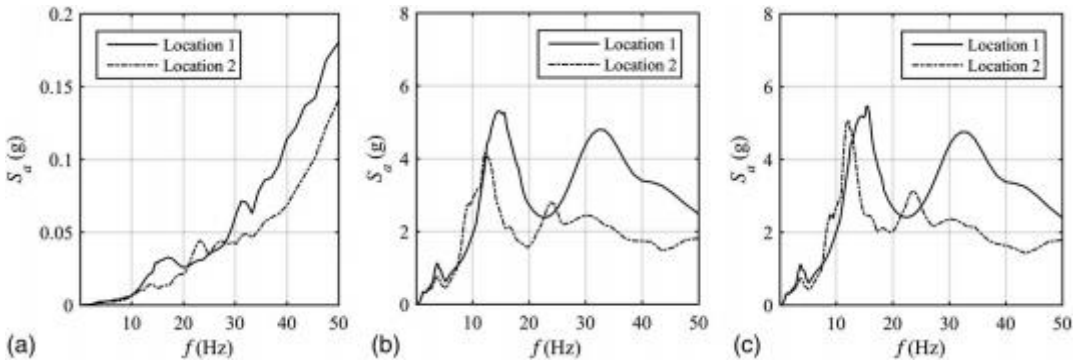

Fig. 14. In-structure response spectra (X direction) at the basemat of the NPP associated with aircraft impact, no SSI: (a) fixed-base; (b) base-isolated (T ¼ 2 s); and (c) base-isolated (T ¼ 3 s).

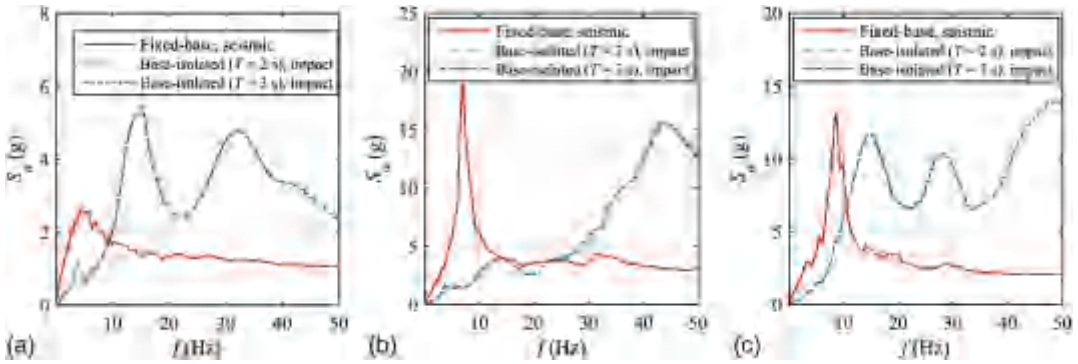

Fig. 15. In-structure response spectra (X direction) in the fixed-base and base-isolated NPPs, no SSI: (a) basemat; (b) containment internal structure; and (c) auxiliary building.

Fig. 16. The isolator response due to aircraft impact is essentially elastic and no energy dissipation is observed. This is primarily due to the relatively large strength of the LR isolation system in the horizontal direction and the large mass of the isolated superstructure.

The effect of isolation-system strength on the response of the NPP due to aircraft impact was investigated by considering an isolation system with a secant period of 3 s and a ratio of strength to supported weight of 0.06 (T3Q6): one half of that considered previously. The properties of the LR bearings in this isolation system (T ¼ 3 s, Q_d=W ¼ 0.06) are presented in Table 1. The choice of characteristic strength, in the practical range considered here, has no meaningful effect on either the acceleration or the displacement response of this base-isolated NPP due to aircraft impact.

The energy histories for aircraft impact and seismic loading of the fixed-base NPP are plotted in Fig. 17. The total energy reported by LS-DYNA is the sum of internal, kinetic, and system damping energy. Energy is considered balanced if the total energy is equal to the sum of external work and initial total energy. LS-DYNA includes stiffness damping energy in internal energy and mass damping is reported separately as system damping energy (Hallquist 2006). The energy is balanced for both analysis cases. The external work (or input energy) by design-basis earthquake shaking is approximately 30 times greater than the work done by aircraft impact.

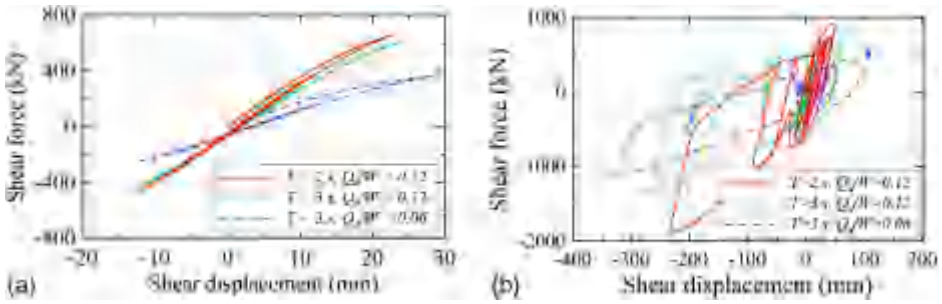

Fig. 16. Horizontal response of the isolator at the center of the basemat of the base-isolated NPPs, no SSI: (a) aircraft impact; and (b) earthquake excitation.

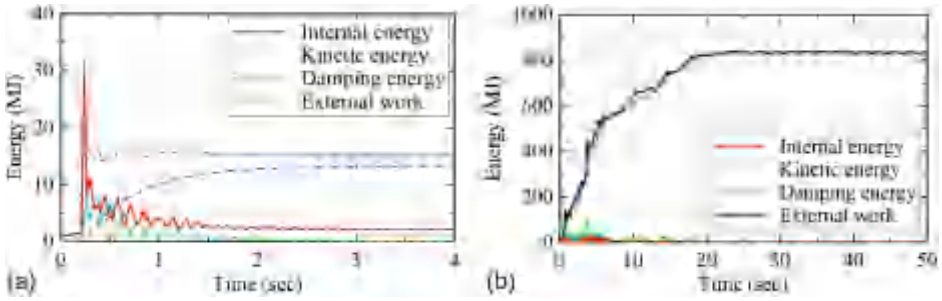

Fig. 17. Energy in the fixed-base NPP subjected to different type of loadings, no SSI: (a) beyond-design-basis aircraft impact; and (b) design-basis earthquake shaking.

Soil-Structure Interaction

Seismic soil-structure interaction (SSI) is analyzed for nearly all NPPs in the United States because the geotechnical media supporting the plant is not rigid and the effect may not be beneficial in terms of reduced in-structure spectral demands. Accordingly, the effects of SSI are calculated here, for a hypothetical soil profile, to identify whether the soil domain should be considered for aircraft impact analysis of NPPs.

There are different strategies for soil-structure interaction analysis in LS-DYNA. The soil domain was modeled here using a perfectly matched layer (PML). The absorbing boundary condition using a PML was implemented in LS-DYNA by Basu (2009), wherein a PML is placed next to an elastic soil domain to absorb the waves passing across the boundary. Reflection from the outer boundary of the PML can be made as small as desired, allowing for accurate modeling of an infinite soil domain using a small elastic medium and a PML layer. The PML layer and the FE model of NPP with soil domain are shown in Figs. 18 and 19, respectively. Three (4.8 m) and five (8 m) layers of finite elements were used for the elastic medium and PML, respectively, beyond the foundation. The dimension of the soil domain was 129.2 × 92.6 × 9.6 m. The size of the soil medium followed the LS-DYNA recommendation (LSTC 2017b) and confirmed by sensitivity analysis.

The elastic properties of the soil domain were back-calculated assuming a shear wave velocity of 760 m=s, which corresponds to the boundary of site classes B and C per ASCE 7-10 (ASCE 2010). The soil domain does not represent any specific site, and variations in mechanical properties with depth were not included because the goal was to qualitatively judge the effect of soil flexibility and damping on the response of the NPP to aircraft impact. Five percent of critical damping was assigned to the elastic soil using the Rayleigh formulation to account for viscous and radiation damping.

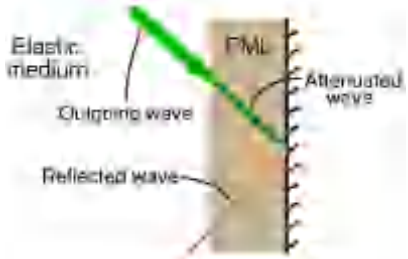

Fig. 18. Modeling of the absorbing soil boundary using perfectly matched layer. (Data from LSTC 2017b.)

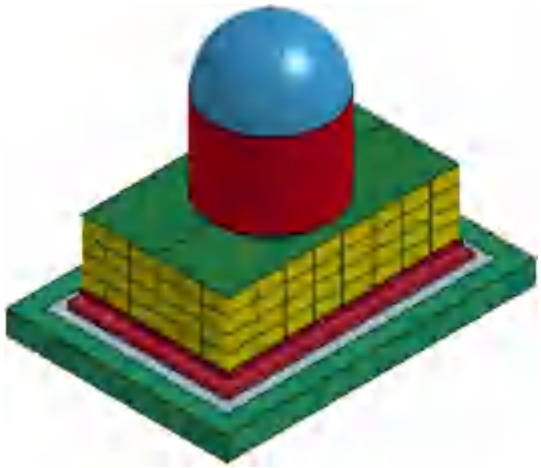

Fig. 19. FE model of a base-isolated NPP including the soil domain.

Table 2. Categorization of passenger aircrafts

Category	Size	Mass range	Models
A	Large	>330 t	A380, A340, B747, B777
B	Intermediate	330–150 t	A300, A330, A350, B767, B707
C	Small	<150 t	A321, B737

Source: Data from Andonov et al. (2010).

Table 3. Soil properties used for soil-structure-interaction analysis

Soil type	Shear wave velocity (m=s)	Elastic modulus ($N=m^2$)	Site period (s)
Interface A-B	1,500	$14{,}493 \times 10^6$	0.026
Interface B-C	760	$3{,}604 \times 10^6$	0.051
Interface C-D	366	836×10^6	0.105

The Rayleigh damping coefficients were obtained using the first and second mode translational periods of the soil column. The effects of soil stiffness and damping are investigated subsequently in the paper. Soil properties are presented in Table 3, including site period, calculated as $4H=\delta 2n - 1 \text{Þ} V_s$, where n is the mode number, H is the thickness of the soil, and V_s is the shear wave velocity in the soil. Poisson's ratio and the density of the soil were assumed to be 0.3 and 2,400 $kg=m^3$, respectively.

The in-structure response of the fixed-base and base-isolated ($T \frac{1}{4} 2$ s, $Q_d=W \frac{1}{4} 0.12$) NPP due to aircraft impact at Location 1, with and without SSI effects, are presented in Figs. 20 and 21, respectively. The soil flexibility dramatically increases in-structure spectral demands at the center of the basemat and at the top of the CIS of the non-isolated NPP because the basemat is put into motion by the impact. The maximum shear strain in the soil was 0.005%: small enough to allow for modeling using linear elastic elements. The effects of SSI on in-structure spectra at the monitoring location in the auxiliary building are tiny. On the basis of the analysis results presented here, ignoring soil flexibility and SSI analysis for aircraft-impact analysis of a fixed-based NPP will underestimate spectral demands at key locations in a NPP. This outcome contrasts sharply with the results of aircraft-impact analysis of the base-isolated NPP, where considerations of soil flexibility result in smaller spectral demands at the center of the basemat.

The effect of soil flexibility on the response of the base-isolated NPP to aircraft impact is investigated by conducting analysis for two additional soil types, namely, described here using shear wave velocities corresponding to the boundaries between site classes: (1) A and B, and (2) C and D. Information on the shear wave velocities, elastic moduli, and site periods for these two cases are provided in Table 3. Results of the analysis are presented in Fig. 22. Greater floor response is observed for the stiffer soil (i.e., A—B) at smaller frequencies, at the basemat of the isolated NPP. The differences in response, at higher locations in the NPP, are negligible.

The sensitivity of the response of the base-isolated NPP to aircraft impact to (1) the assumed damping formulation; and (2) the assigned value of damping in the soil is investigated next. Floor spectra were generated for four damping formulations, namely, (1) mass proportional, (2) stiffness proportional, (3) Rayleigh,

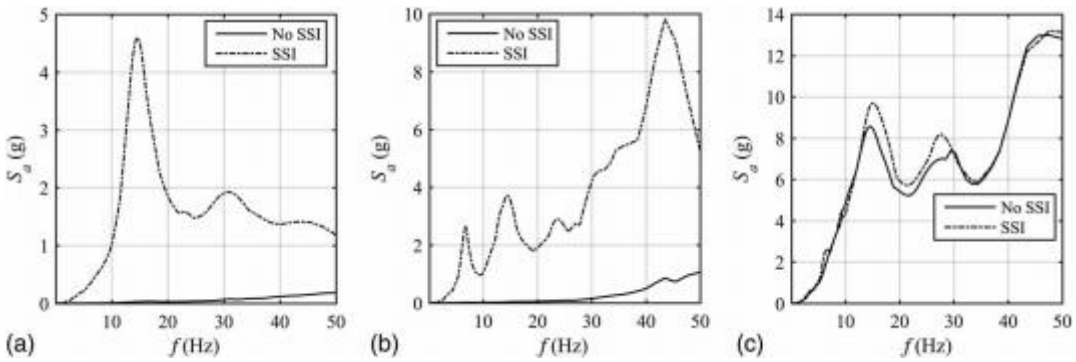

Fig. 20. In-structure response spectra (X direction) in a non-isolated NPP due to aircraft impact, including SSI, soil type BC: (a) basemat; (b) containment internal structure; and (c) auxiliary building.

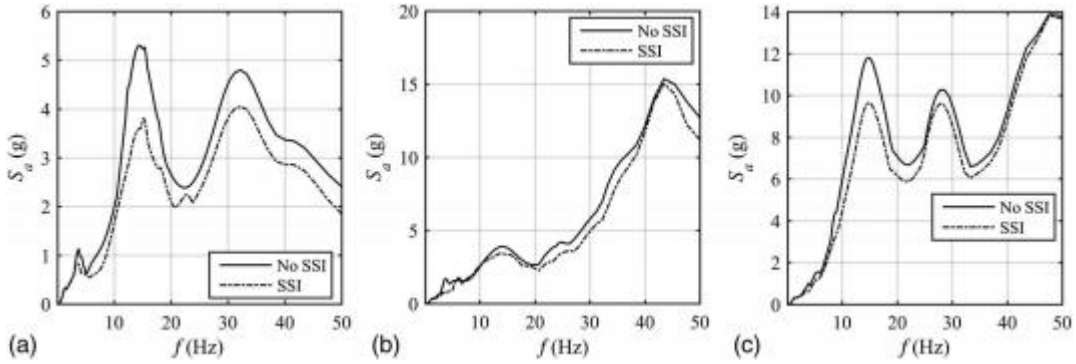

Fig. 21. In-structure response spectra (X direction) in an isolated NPP due to aircraft impact, including SSI, soil type BC: (a) basemat; (b) containment internal structure; and (c) auxiliary building.

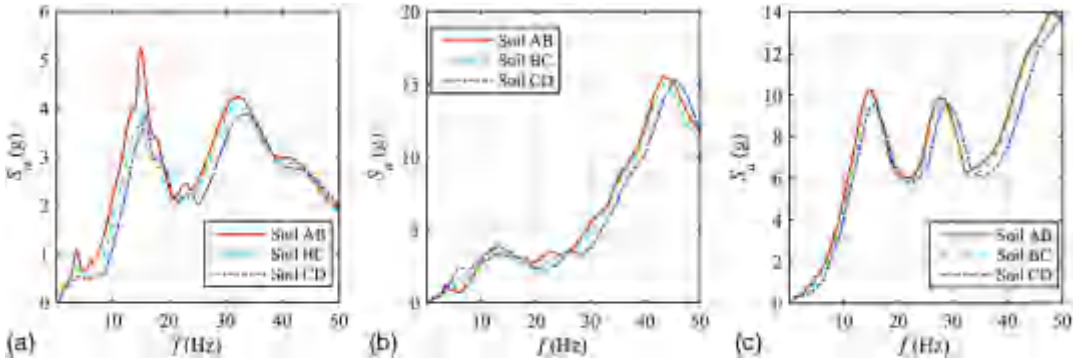

Fig. 22. In-structure response spectra (X direction) in an isolated NPP due to aircraft impact, including SSI, three soil types, 5% soil damping: (a) basemat; (b) containment internal structure; and (c) auxiliary building.

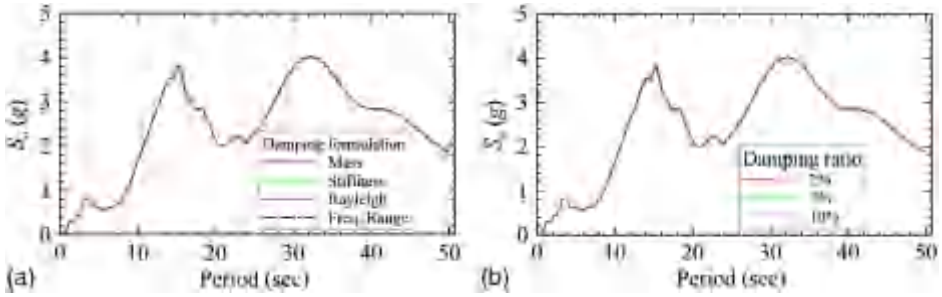

Fig. 23. In-structure response spectra (X direction) at the basemat of an isolated NPP due to aircraft impact, including SSI: (a) damping formulation; and (b) damping value.

and (4) uniform frequency damping and 5% of critical damping. The proportionality constants for the first three formulations were obtained using the first two periods of the soil domain. Floor responses were also obtained using the Rayleigh formulation and 2, 5, and 10% damping in the soil. Small values of damping are considered here because the expected shear strains in the soil are small. The ordinates of the in-structure response spectra are not sensitive to either the chosen damping formulation or the value of soil damping (in the range considered), as shown in Fig. 23.

Summary and Conclusions

A testbed NPP was analyzed to judge whether the implementation of a base-isolation system for enhanced protection under design-basis and beyond-design-basis earthquake shaking would compromise the performance of structures, systems, and components in the building for beyond-design-basis aircraft impact. The testbed NPP was a generic large light water reactor. The impacting aircraft was a large commercial airliner and the impact velocity was high and normal to the CCV. The performance of the NPP was measured using in-structure (floor) response spectra. Lateral displacements in the seismic isolation system were calculated and reported. Local damage to the CCV due to impact was not addressed because (1) it would affect neither the response of the isolation system nor the in-structure response spectra remote from the point of impact; and (2) reinforcement details for the CCV were not available.

A detailed FE model of the NPP was built in LS-DYNA and the impact loading function was described by a Riera function. Linear behavior was assumed for the NPP and the supporting soil (where modeled). Nonlinear models were used for the seismic isolators. Two locations of impact on the CCV were considered. The effects of isolator mechanical properties, soil-structure interaction, and chosen values of soil stiffness and damping on the response due to aircraft impact were investigated.

The key conclusions of the study described in this paper are the following:

1. In-structure spectral demands due to aircraft impact in a base-isolated NPP will be greater than those in its fixed-base counterpart on rigid rock because the isolated basemat is put into motion.
2. The peak floor spectral acceleration in a base-isolated NPP due to aircraft impact is smaller than that due to design-basis shaking of the corresponding fixed-base NPP, founded on rock, at frequencies less than 10 Hz.
3. Structures, systems, and components in an NPP may experience spectral demands at high frequencies for beyond-design-basis aircraft impact that are greater than those for design-basis earthquake shaking, regardless of whether the NPP is base isolated.
4. In-structure spectral demands due to aircraft impact in a base-isolated NPP are insensitive to the secant period and/or characteristic strength of an isolation system, for the range of isolator properties considered here.
5. The response of the isolation system due to impact of a large commercial aircraft is essentially elastic for the NPP of the size and mass considered here. Consequently, damping in an isolator does not significantly affect the response of a NPP due to aircraft impact.
6. The inclusion of a compliant soil domain beneath the NPP will lead to higher in-structure spectral demands than those in the fixed-base counterpart founded in rock because the basemat is put into motion: soil—structure interaction. The effect of soil—structure interaction on the response of an isolated NPP due to aircraft impact is relatively small.

These conclusions are somewhat specific to the assumed NPP, design seismic hazard, foundation condition (soil type), aircraft, and impact velocity. A reduction in the mass of the NPP will lead to increased in-structure response in both the base-isolated NPP and in the conventionally founded NPP founded on a compliant soil. A reduction in the size of the aircraft and/or the impact velocity will reduce in-structure response in all cases, for the same location of impact.

Acknowledgments

Financial support for this research project was provided by the United States Nuclear Regulatory Commission (USNRC) through a grant to MCEER via a contract led by Dr. Robert Budnitz at the Lawrence Berkeley National Laboratory (LBNL). The authors acknowledge the technical contributions of the Dr. Budnitz, the LBNL review panel, and Dr. Jose Pires of the USNRC to this research project.

References

Andonov, A., K. Apostolov, D. Stefanov, and M. Kostov. 2009. "On the floor response spectra due to aircraft impact." In Proc., 20th Int. Conf. on Structural Mechanics in Reactor Technology (SMiRT 20). Raleigh, NC: International Association for Structural Mechanics in Reactor Technology.

Andonov, A., K. Apostolov, D. Stefanov, and M. Kostov. 2010. "Parametric study on the floor response spectra and the damage potential of aircraft impact induced vibratory loading." J. Disaster Res. 5 (4): 417–425. https://doi.org/10.20965/jdr.2010.p0417.

Arros, J., and N. Doumbalski. 2007. "Analysis of aircraft impact to concrete structures." Nucl. Eng. Des. 237 (12): 1241–1249. https://doi.org/10.1016/j.nucengdes.2006.09.044.

ASCE. 2010. Minimum design loads for buildings and other structures. ASCE/SEI Standard 7-10. Reston, VA: ASCE.

Basu, U. 2009. "Explicit finite element perfectly matched layer for transient three-dimensional elastic waves." Int. J. Numer. Methods Eng. 77 (2): 151–176. https://doi.org/10.1002/nme.2397.

Hallquist, J. O. 2006. LS-DYNA theory manual. Livermore, CA: Livermore Software Technology Corporation.

Iliev, A., A. Andonov, and M. Kostov. 2013. "Limitations of the load time function approach for assessment of complex structures." In Proc., 22nd Int. Conf. on Structural Mechanics in Reactor Technology (SMiRT 22). Raleigh, NC: International Association for Structural Mechanics in Reactor Technology.

Iliev, V., K. Georgiev, and V. Serbezov. 2011. "Assessment of impact load curve of Boeing 747-400." Mach. Technol. Mater. Int. Sci. J. 1 (1): 22–25.

Keldrauk, E., P. F. Peterson, and B. Stojadinovic. 2011. "Framework for performance-based evaluation and design of seismic isolation for nuclear energy facility structures." In Proc., 21st Int. Conf. on Structural Mechanics in Reactor Technology (SMiRT-21). Raleigh, NC: International Association for Structural Mechanics in Reactor Technology.

Kirkpatrick, S. W., R. MacNeill, R. T. Bocchieri, V. Phan, R.-Y. Jung, and J. Lee. 2013. "Evaluation of aircraft impact analysis methodologies for nuclear safety applications." In Proc., 22nd Int. Conf. on Structural Mechanics in Reactor Technology (SMiRT 22). Raleigh, NC: International Association for Structural Mechanics in Reactor Technology.

Kostov, M., A. Iliev, and A. Andonov. 2013. "Load time function defintion for large commercial aircraft impact: Parametric study." In Proc., 22nd Int. Conf. on Structural Mechanics in Reactor Technology (SMiRT 22). Raleigh, NC: International Association for Structural Mechanics in Reactor Technology.

Kulak, R. F., and B. Yoo. 2003. "Effects of aircraft impact on a seismically isolated reactor building." Proc., 17th Int. Conf. on Structural Mechanics in Reactor Technology (SMiRT-17). Raleigh, NC: International Association for Structural Mechanics in Reactor Technology.

Kumar, M., and A. Whittaker. 2017. "Cross-platform implementation, verification and validation of advanced mathematical models of elastomeric seismic isolation bearings." Eng. Struct., in press.

Kumar, M., A. Whittaker, and M. Constantinou. 2014. "An advanced numerical model of elastomeric seismic isolation bearings." Earthquake Eng. Struct. Dyn. 43 (13): 1955–1974. https://doi.org/10.1002/eqe.2431.

Kumar, M., A. Whittaker, and M. Constantinou. 2015a. "Characterizing friction in sliding isolation bearings." Earthquake Eng. Struct. Dyn. 44 (9): 1409–1425. https://doi.org/10.1002/eqe.2524.

Kumar, M., A. Whittaker, and M. Constantinou. 2015b. "Experimental investigation of cavitation in elastomeric seismic isolation bearings." Eng. Struct. 101: 290–305. https://doi.org/10.1016/j.engstruct.2015.07.014.

Kumar, M., A. Whittaker, and M. Constantinou. 2015c. "Response of base-isolated nuclear structures to extreme earthquake shaking." Nucl. Eng. Des. 295: 860–874. https://doi.org/10.1016/j.nucengdes.2015.06.005.

Kumar, M., A. S. Whittaker, and M. C. Constantinou. 2015d. Seismic isolation of nuclear power plants using elastomeric bearings. Technical Rep. MCEER-15-0008. New York: Univ. at Buffalo.

Kumar, M., A. S. Whittaker, and M. C. Constantinou. 2015e. Seismic isolation of nuclear power plants using sliding bearings. Technical Rep. MCEER-15-0006. New York: Univ. at Buffalo.

LSTC (Livermore Software Technology Corporation). 2016. "Damping in LS-DYNA." Accessed November 1, 2016. http://www.dynasupport.com/howtos/general/damping.

LSTC (Livermore Software Technology Corporation). 2017a. LS-DYNA keyword user's manual. Livermore, CA: LSTC.

LSTC (Livermore Software Technology Corporation). 2017b. "PML absorbing boundary." Accessed April 1, 2017. http://www.lstc.com/applications/soil_structure/pml.

Nagarajaiah, S., A. M. Reinhorn, and M. C. Constantinou. 1989. Nonlinear dynamic analysis of three-dimensional base-isolated structures (3D-BASIS). Technical Rep. NCEER-89-0019. New York: Univ. at Buffalo.

Orr, R. 2003. AP1000 inputs for 2D SASSI analyses. Cranberry Township, PA: Westinghouse Electric Company.

Park, Y. J., Y. K. Wen, and A. H. S. Ang. 1986. "Random vibration of hysteretic systems under bi-directional ground motions." Earthquake Eng. Struct. Dyn. 14 (4): 543–557. https://doi.org/10.1002/eqe.4290140405.

Riera, J. D. 1968. "On the stress analysis of structures subjected to aircraft impact forces." Nucl. Eng. Des. 8 (4): 415–426. https://doi.org/10.1016/0029-5493(68)90039-3.

Riera, J. D. 1980. "A critical reappraisal of nuclear power plant safety against accidental aircraft impact." Nucl. Eng. Des. 57 (1): 193–206. https://doi.org/10.1016/0029-5493(80)90233-2.

USNRC (Nuclear Regulatory Commission). 1998a. 10 CFR Part 50—Domestic licensing of production and utilization facilities. Washington, DC: USNRC.

USNRC (Nuclear Regulatory Commission). 1998b. 10 CFR Part 52—Licenses, certifications, and approvals for nuclear power plants. Washington, DC: USNRC.